Journal of Inflammation Research

Dovepress
Taylor & Francis Group

Open Access Full Text Article

ORIGINAL RESEARCH

Identification and Validation of Feature Genes Related to Mitochondrial Dysfunction and Oxidative Stress in Ulcerative Colitis

Yanrui Wu[1,*], Zongbiao Tan[1,*], Qingzhi Lan[2,*], Yupei Liu[1], Chuan Liu[1], Haodong He[1], Jixiang Zhang[1], Weiguo Dong[1]

[1]Department of Gastroenterology, Renmin Hospital of Wuhan University, Wuhan, People's Republic of China; [2]Department of Pathology, Renmin Hospital of Wuhan University, Wuhan, People's Republic of China

*These authors contributed equally to this work

Correspondence: Weiguo Dong, Department of Gastroenterology, Renmin Hospital of Wuhan University, 99 Zhangzhidong Road, Wuhan, Hubei Province, 430060, People's Republic of China, Email dongweiguo@whu.edu.cn

Background: The roles of mitochondrial dysfunction (MD) and oxidative stress (OS) in the pathogenesis of ulcerative colitis (UC) have received increasing attention. Given their close association, it is crucial to clarify the molecular characteristics and biological functions of MD and OS-related genes in UC.

Methods: Gene expression profiles, mitochondrial-related genes, and OS-related genes were obtained from the corresponding databases. Unsupervised clustering of UC samples was performed based on differentially expressed MD and OS-related genes (DEMORGs). The CIBERSORT algorithm was used to assess immune cell infiltration. Feature genes were selected from DEMORGs by machine learning. The receiver operating characteristic (ROC) curves were plotted, and a nomogram was constructed to evaluate the diagnostic efficacy of feature genes for UC. Colonoscopic biopsy tissues from UC patients and controls were collected retrospectively to verify the protein expression levels of feature genes through immunohistochemical staining.

Results: Based on nine DEMORGs, two MD and OS-related subtypes were identified in UC samples. Subtype C2 is characterized by a more severe degree of MD, higher OS levels, and more severe disease activity. The infiltration proportions of follicular helper T cells, M1 macrophages, activated dendritic cells, and neutrophils were significantly higher in subtype C2 compared to subtype C1. CPT1A, EPHX2, and PRDX4 were obtained as UC feature genes related to MD and OS. All the three feature genes exhibited good diagnostic value for UC, and their expression levels were significantly correlated with the clinical activity of UC.

Conclusion: CPT1A, EPHX2, and PRDX4 are feature genes related to MD and OS in UC, and their expression levels are significantly associated with the proportion of immune cell infiltration and disease activity. This study provides valuable insights into the role of MD and OS in UC.

Keywords: ulcerative colitis, mitochondrial dysfunction, oxidative stress, bioinformatics analysis, machine learning

Introduction

Ulcerative colitis (UC) is an inflammatory bowel disease (IBD) primarily affecting the rectal and colonic mucosa, typically with clinical manifestations of hematochezia and diarrhea.[1] The pathogenesis of UC is complex and incompletely understood. At present, it is thought to involve genetic susceptibility, environmental factors, impaired intestinal epithelial barrier, immune dysregulation, and gut microbiota imbalance.[2] Since UC is incurable and characterized by a course of relapses and remissions, it severely impacts patients' quality of life and places a heavy burden on healthcare systems.[3] Currently, the therapeutic goal of UC is to induce and maintain remission, and therapeutic agents mainly include aminosalicylic acid preparations, glucocorticoids, immunomodulators, and biological agents.[4] The advent of biological agents, which target inflammatory factors or signal transduction molecules, has undoubtedly been a boon to

Received: 16 November 2024
Accepted: 15 April 2025
Published: 30 April 2025

patients with UC, but the overall remission rate is still limited.[5] Thus, there is an urgent need to further understand the pathogenesis of UC to identify more biomarkers and treatment strategies.

In recent years, increasing attention has been paid to the role of mitochondrial dysfunction (MD) in the pathogenesis of UC. Studies have shown that colonic epithelial cells in UC patients exhibit structural and functional abnormalities in mitochondria, such as mitochondrial swelling, loss of cristae structure, and decreased activity of electron transport chain (ETC) complexes.[6,7] Cunningham et al found that the expression of peroxisome proliferator-activated receptor γ coactivator 1α (PGC1α), a key regulator of mitochondrial biogenesis, was reduced in the intestinal tissues of UC patients and colitis mice.[8] They further revealed that PGC1α downregulation exacerbates colitis by impairing mitochondrial homeostasis and intestinal barrier function.[8] Additionally, high levels of mitochondrial DNA (mtDNA) can be detected in the plasma and feces of UC patients, and these levels are significantly correlated with inflammatory markers and disease activity.[6] mtDNA is considered a type of damage-associated molecular pattern (DAMP) released following mitochondrial injury, which can be recognized by intracellular pattern recognition receptors (PRRs), thereby triggering a cascade of inflammatory and immune responses.[9] MD can also influence the phenotype and function of immune cells through metabolic reprogramming, leading to the maintenance of a pro-inflammatory state.[10]

Mitochondria are the primary source of reactive oxygen species (ROS) within cells.[11] Under physiological conditions, the antioxidant defense system maintains ROS at low levels, enabling their beneficial roles in signal transduction, immune defense, and metabolic adaptation.[12] During MD, factors such as decreased activity of ETC complexes and abnormal mitophagy lead to a pathological elevation of ROS levels.[13] Once these levels exceed the clearing capacity of the antioxidant defense system, oxidative stress (OS) can occur. In UC, a deficiency in intestinal mucosal antioxidant defense is also a contributing factor to OS, such as the reduced expression or dysfunction of nuclear factor E2-related factor 2 (Nrf2). Nrf2 is a transcription factor that induces the production of various antioxidant enzymes and plays a critical role in oxidative defense.[14] OS can accelerate cellular damage through protein modifications and lipid peroxidation, while also upregulating pro-inflammatory signaling pathways and disrupting tight junctions in intestinal epithelial cells (IECs).[15] Recent research has also revealed that OS drives intestinal inflammation by activating mitochondria-dependent necroptosis.[16] More importantly, OS aggravates MD through multiple mechanisms, including mtDNA damage, disruption of mitochondrial membrane structure, and impairment of ETC function, ultimately establishing a vicious cycle between MD and OS.[17] Therefore, it is essential to clarify the molecular characteristics and biological functions of MD and OS-related genes in UC. Most current studies focus only on a single factor,[18,19] with limited research combining both aspects.

The application of microarray technology, bioinformatics analysis, and machine learning has made the screening of disease characteristic molecules and the search for therapeutic targets more precise. In this study, we integrated bioinformatics analysis and machine learning methods to mine gene expression data selected from the Gene Expression Omnibus (GEO), to reveal the association between MD and OS-related genes and immune cell infiltration, identify MD and OS-related feature genes, and explore their clinical significance in UC. The flowchart of this study is presented in Figure 1.

Methods

Data Sources

The gene expression profiles of intestinal mucosal biopsy samples were obtained from GEO (https://www.ncbi.nlm.nih.gov/geo/), including the training set (GSE92415)[20] and the validation set (GSE206285),[21] both of which are annotated by the GPL13158 platform. GSE92415 included 87 UC patients prior to treatment with golimumab or placebo, along with 21 healthy controls (HC), while GSE206285 consisted of 550 UC patients and 18 healthy subjects. A total of 1,136 mitochondrial-related genes (MRGs) were downloaded from the Human MitoCarta3.0 database (https://www.broadinstitute.org/mitocarta/). Using the term "oxidative stress", 401 oxidative stress-related genes (OSRGs) were retrieved from the Molecular Signatures Database (MSigDB) (http://www.gsea-msigdb.org/gsea/downloads.jsp), and 990 OSRGs were identified from the GeneCards database (https://www.genecards.org/) based on a relevance score>8, resulting in a final set of 1,139 OSRGs. Details of MRGs and OSRGs are provided in Supplementary Table 1.

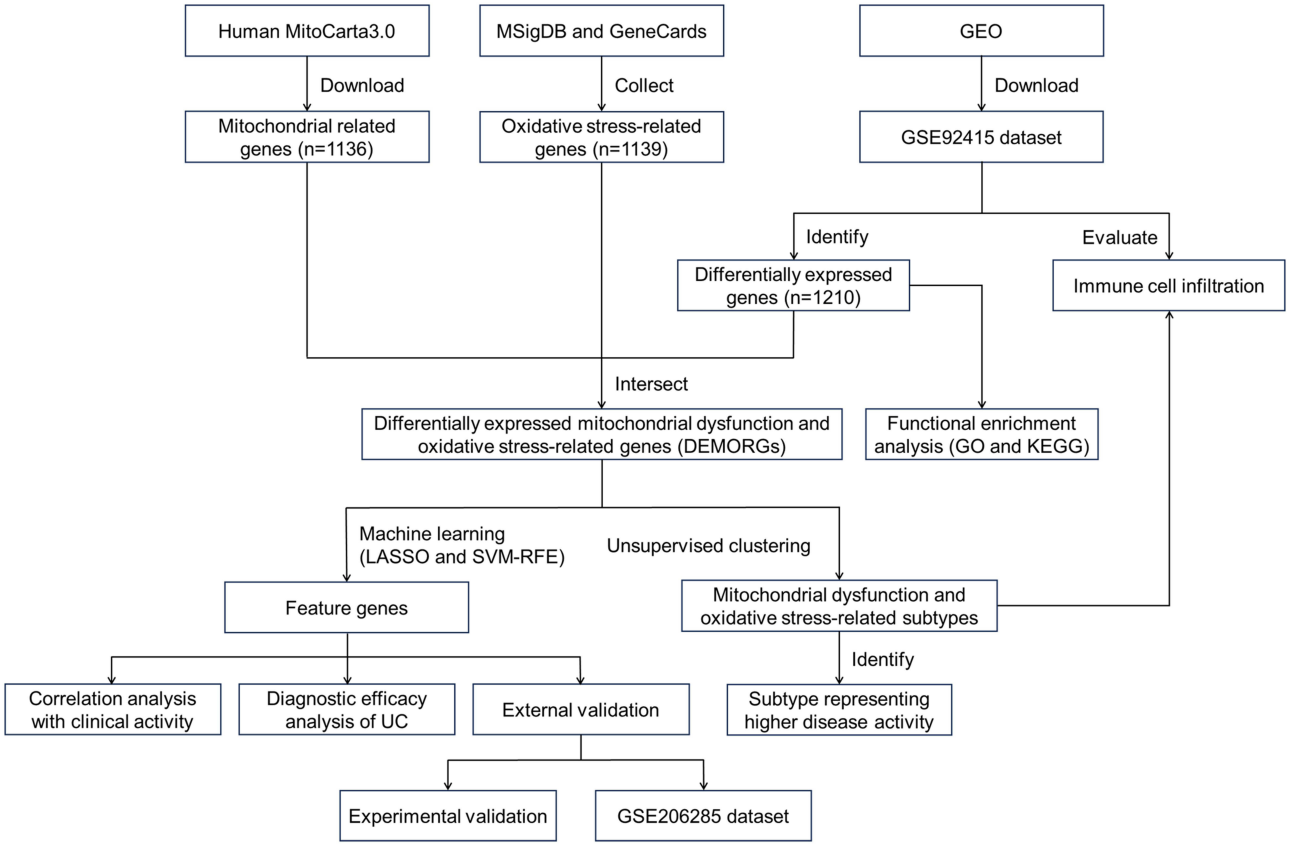

Figure 1 Flowchart of the study.
Abbreviations: MSigDB, Molecular Signatures Database; GEO, Gene Expression Omnibus; GO, Gene Ontology; KEGG, Kyoto Encyclopedia of Genes and Genomes; LASSO, Least Absolute Shrinkage and Selection Operator; SVM-RFE, Support Vector Machine-Recursive Feature Elimination; UC, ulcerative colitis.

Identification and Functional Enrichment Analysis of Differentially Expressed Genes (DEGs)

Using |log2(Fold Change)|>1 and adjusted *P*-value<0.05 as criteria, DEGs between UC and HC were identified in the GSE92415 dataset using the "limma" package, and heatmaps and volcano plots were generated with the "pheatmap" and "ggplot2" packages, respectively. Subsequently, Gene Ontology (GO) and Kyoto Encyclopedia of Genes and Genomes (KEGG) enrichment analyses were performed on DEGs using the "clusterProfiler" package. GO analysis was used for biological function annotation, including biological process (BP), cellular component (CC), and molecular function (MF). KEGG analysis explored the signaling pathways that DEGs may be involved in.

Identification of MD and OS-Related Subtypes

The intersection of DEGs, MRGs, and OSRGs represents the differentially expressed MD and OS-related genes (DEMORGs). And the correlations among DEMORGs can be visualized by the "corrplot" package. Based on the expression data of DEMORGs, unsupervised clustering of UC samples was performed using the "ConsensusClusterPlus" package to identify different MD and OS-related subtypes. The expression levels of DEMORGs, mitochondrial function scores, and disease activity were compared between subtypes to identify the characteristics of each UC subtype. Mitochondrial function scores for each UC sample were calculated using MRGs through Gene Set Variation Analysis (GSVA), and disease activity was measured by the Mayo score.

https://doi.org/10.2147/JIR.S506851

Assessment of Immune Cell Infiltration

CIBERSORT is one of the most widely used methods for assessing immune cell infiltration. We used the CIBERSORT algorithm to infer the infiltration proportions of 22 types of immune cells from gene expression profiles and visualized the differences in immune cell infiltration between UC and HC, as well as between different UC subtypes, using boxplots created with the "ggplot2" package. Simultaneously, a correlation analysis was conducted between the expression of DEMORGs and the infiltration proportions of immune cells.

Machine Learning Screening for Feature Genes

Least Absolute Shrinkage and Selection Operator (LASSO) and Support Vector Machine-Recursive Feature Elimination (SVM-RFE) are commonly used machine learning algorithms for selecting feature genes. LASSO regression is a regularized linear regression method that reduces model complexity and selects important features, while SVM-RFE is a feature selection algorithm that progressively removes unimportant features using an SVM model. The two algorithms were used separately to filter DEMORGs, and the intersection was taken to obtain MD and OS-related feature genes.

Diagnostic Efficacy Analysis of Feature Genes

The "pROC" package was used to plot the receiver operating characteristic (ROC) curves for each feature gene and calculate the area under the curve (AUC), while validation was conducted in the GSE206285 dataset. Furthermore, a diagnostic nomogram for UC was generated using the "rms" package, and its predictive performance was evaluated through ROC curve, calibration curve, and decision curve analysis (DCA).

Correlation Analysis Between Feature Genes and Disease Activity

Spearman correlation coefficients and *P*-values between the expression of each feature gene and disease activity (represented by the Mayo score) were calculated among UC patients in the GSE92415 dataset. Changes in the expression of feature genes before and after treatment with biological agents were also compared. Among UC patients treated with golimumab, 42 had gene expression profiles at weeks 0 and 6, including 24 responders and 18 non-responders at week 6.

Collection of Clinical Samples

In this study, the clinical data and colonoscopic biopsy paraffin sections of 10 patients with active UC and 5 healthy subjects who were hospitalized in the Department of Gastroenterology, Renmin Hospital of Wuhan University from October 2022 to May 2023 were retrospectively collected. All included patients with a clear diagnosis of UC were supported by clinical symptoms, endoscopic manifestations, and pathological characteristics. This study has been approved by the Ethics Committee of Renmin Hospital of Wuhan University (WDRY 2022-K130), and all participants have signed an informed consent form.

Immunohistochemical Staining

After paraffin sections were deparaffinized with xylene and hydrated with graded concentrations of ethanol, high-pressure antigen retrieval was performed with citrate repair solution, and 3% H_2O_2 solution was prepared to inactivate endogenous peroxidases. Subsequently, the sections were blocked with 10% goat serum and incubated overnight at 4°C with specific concentrations of primary antibodies (Supplementary Table 2). The next day, the sections were washed and incubated with horseradish peroxidase-labeled secondary antibody for 1 hour and color developed with diaminobenzidine (DAB). Finally, the nuclei were counterstained with hematoxylin, and the images were acquired using a slide scanning system after the sealing was completed. For each slide, three random fields were selected at 400× magnification, and the average optical density (AOD) was calculated using Image J software for statistical analysis.

Statistical Analysis

All bioinformatics and statistical analyses in this study were conducted in R software (version 4.4.0). Comparisons between two groups were performed using the *t*-test or Wilcoxon test, while paired samples were analyzed using the

paired *t*-test. Correlations between variables were assessed by calculating the Spearman correlation coefficient. All statistical tests were two-sided, and *P* values less than 0.05 were considered statistically significant.

Results

DEGs were Significantly Enriched in Biological Functions and Signaling Pathways Related to Inflammation and Immunity

A total of 1,210 DEGs were identified between UC and HC, including 808 upregulated genes and 402 downregulated genes (Figure 2A and B). GO analysis revealed that DEGs were significantly enriched in BP (such as response to lipopolysaccharide and leukocyte migration) and MF (such as cytokine activity and receptor binding) related to inflammatory response and immune regulation (Figure 2C). KEGG analysis demonstrated that DEGs were significantly enriched in multiple classic inflammatory and immune signaling pathways, including the TNF signaling pathway, IL-17 signaling pathway, and NF-κB signaling pathway (Figure 2D).

Nine DEMORGs Were Identified

The intersection of 1,136 MRGs and 1,139 OSRGs yielded 252 genes related to MD and OS. These 252 genes were further intersected with DEGs, and nine DEMORGs were finally obtained, which were ETFDH, CPT2, ACADS, SOD2, PDK2, CPT1A, EPHX2, MAOA, and PRDX4 (Figure 2E). The correlations among DEMORGs are shown in Figure 2F, where PRDX4 is positively correlated with SOD2, but both genes are negatively correlated with the remaining seven genes.

Two MD and OS-Related Subtypes Were Identified in UC Patients

Unsupervised clustering was conducted on 87 UC patients in the GSE92415 dataset based on the nine DEMORGs. As shown in Figure 3A, the consistency score of the clustering was optimal when the number of clusters "k" was set to 2. Therefore, the UC patients were categorized into two MD and OS-related subtypes, with 45 cases in subtype C1 and 42 cases in subtype C2. The consistency matrix heatmap, principal component analysis (PCA) plot, and gene expression heatmap further verified the stability of the clustering results (Figure 3B–D). Comparing subtypes C1 and C2, we found no significant age difference between the two subtypes (P=0.400), whereas subtype C2 had lower mitochondrial function scores and higher Mayo scores (both P<0.05) (Figure 3E–G). Regarding gene expression, the expression of SOD2 and PRDX4 in subtype C2 was significantly higher than that in subtype C1 (both P<0.001), while the expression of ETFDH, CPT2, ACADS, PDK2, CPT1A, EPHX2, and MAOA was significantly lower in subtype C2 (all P<0.001) (Figure 3H). Therefore, subtype C2 is characterized by a more severe degree of MD, higher OS levels, and more severe disease activity.

There Were Significant Differences in Immune Cell Infiltration Between the Two Subtypes

As shown in Figure 4A and B, among the 22 immune cell types evaluated by CIBERSORT, the infiltration proportions of follicular helper T (Tfh) cells, M1 macrophages, activated dendritic cells (DCs), and neutrophils were significantly higher in the UC group compared to the HC group (all P<0.001), and were significantly higher in subtype C2 than in subtype C1 (all P<0.05). In contrast, the infiltration proportions of $CD8^+$ T cells, activated NK cells, M2 macrophages, and resting mast cells were significantly lower in the UC group compared to the HC group (all P<0.05), and were also significantly lower in subtype C2 than in subtype C1 (all P<0.05). Among the nine DEMORGs, the expression of SOD2 and PRDX4 was positively correlated with the infiltration proportion of elevated immune cells in the UC group/subtype C2, and negatively correlated with the infiltration proportion of decreased immune cells in the UC group/subtype C2; while the other seven genes exhibited the opposite pattern (Figure 4C).

Three UC Feature Genes Related to MD and OS Were Identified Through Machine Learning

Four genes (ETFDH, CPT1A, EPHX2, and PRDX4) were screened from DEMORGs by LASSO regression. Meanwhile, four genes (CPT1A, PRDX4, SOD2, and EPHX2) were also identified using SVM-RFE algorithm. The results of

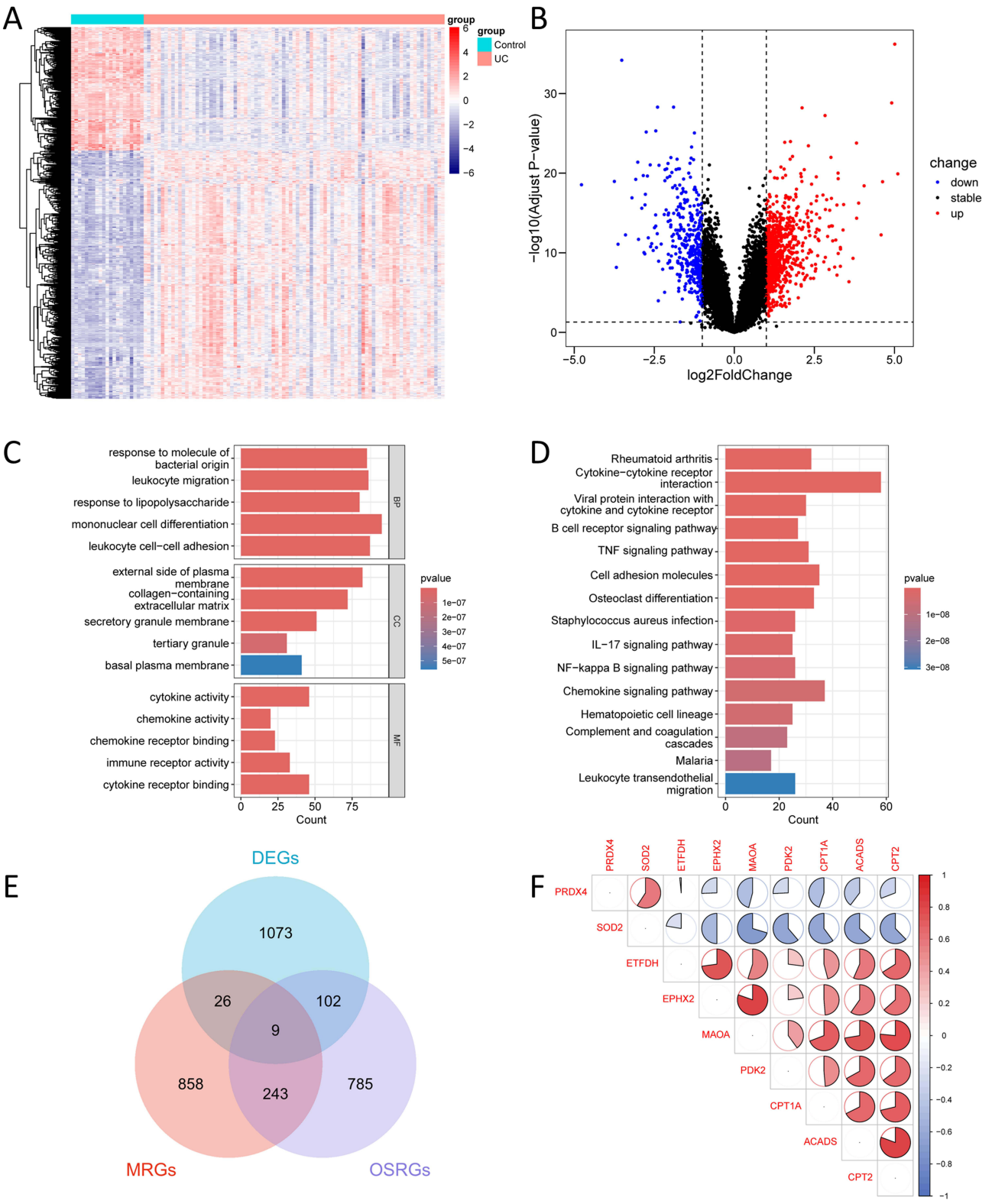

Figure 2 Identification of DEGs and DEMORGs. (**A**) Heatmap of DEGs between UC patients and healthy controls. (**B**) Volcano plot of DEGs between UC patients and healthy controls. (**C**) Results of GO enrichment analysis of DEGs. (**D**) Results of KEGG enrichment analysis of DEGs. (**E**) Venn diagram: the intersection of DEGs, MRGs, and OSRGs is DEMORGs. (**F**) Heatmap of correlations among DEMORGs (Spearman correlation coefficient).

Abbreviations: DEGs, differentially expressed genes; DEMORGs, differentially expressed mitochondrial dysfunction and oxidative stress-related genes; UC, ulcerative colitis; GO, Gene Ontology; KEGG, Kyoto Encyclopedia of Genes and Genomes; BP, biological process; CC, cellular component; MF, molecular function; MRGs, mitochondrial-related genes; OSRGs, oxidative stress-related genes.

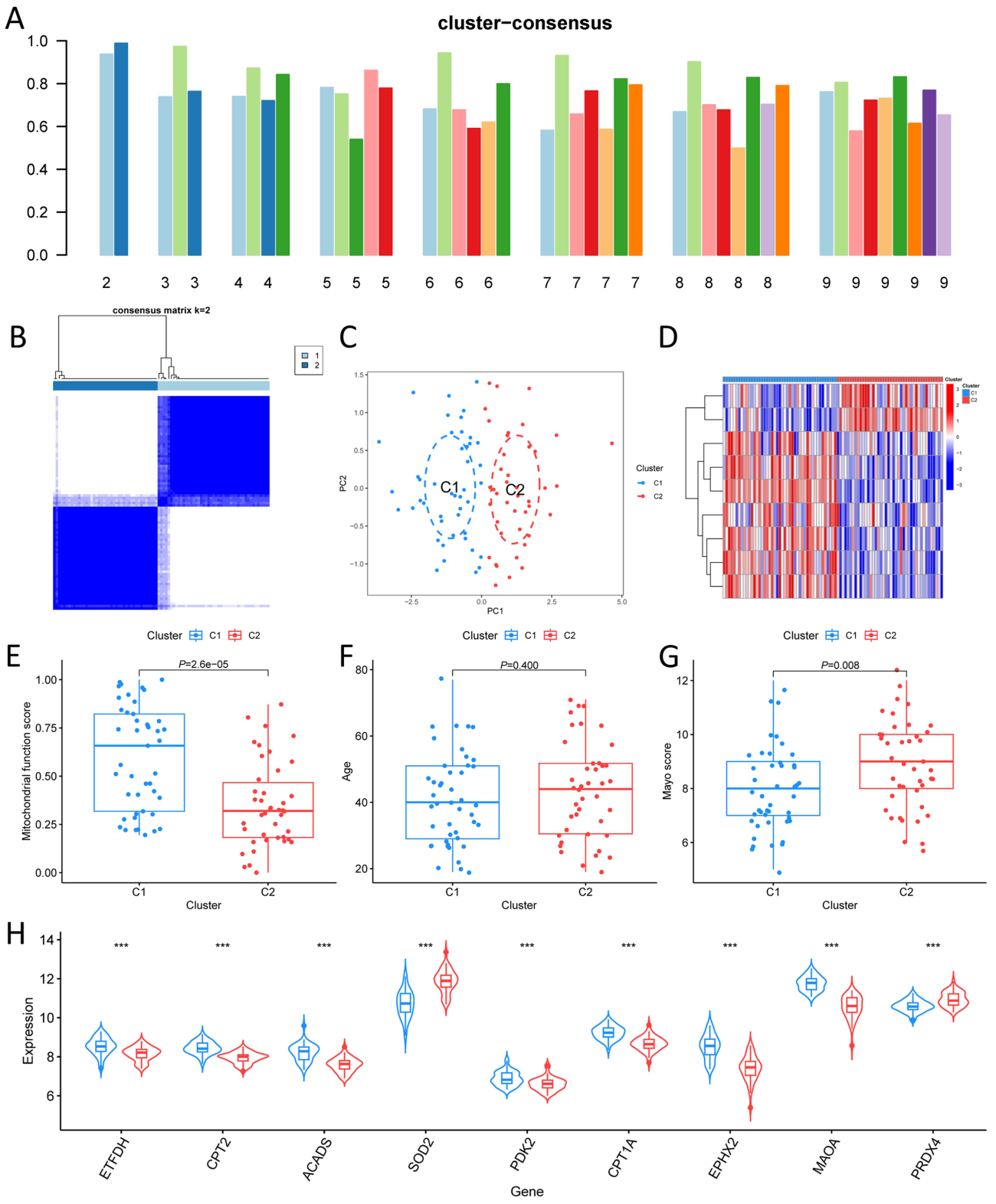

Figure 3 Identification of MD and OS-related subtypes. (**A**) Consistency scores for unsupervised clustering when the number of clusters "k" is taken as 2–9. (**B**) Consensus matrix heatmap when k=2. (**C**) Principal component analysis plot. (**D**) Gene expression heatmap. (**E-G**) Boxplots comparing mitochondrial function scores, age, and Mayo scores between subtypes C1 and C2 (median [IQR], Wilcoxon test). (**H**) Violin plot comparing the expression levels of DEMORGs between subtypes C1 and C2 (median [IQR], Wilcoxon test). ***P<0.001.

Abbreviations: MD, mitochondrial dysfunction; OS, oxidative stress; IQR, interquartile range; DEMORGs, differentially expressed MD and OS-related genes.

https://doi.org/10.2147/JIR.S506851

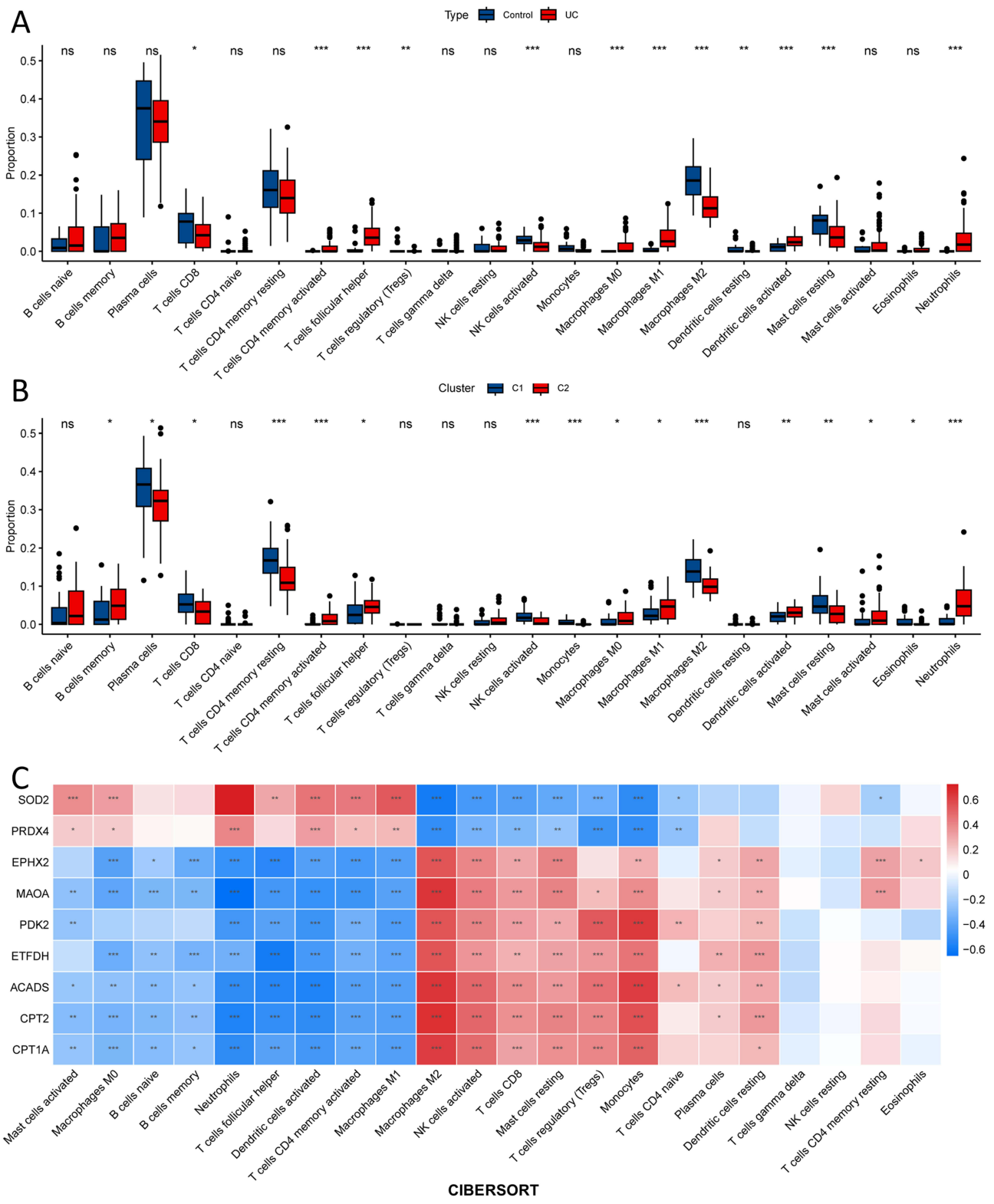

Figure 4 Assessment of immune cell infiltration. (**A**) Boxplot comparing the infiltration proportions of 22 types of immune cells between UC patients and healthy controls (median [IQR], Wilcoxon test). (**B**) Boxplot comparing the infiltration proportions of 22 types of immune cells between subtypes C1 and C2 (median [IQR], Wilcoxon test). (**C**) Heatmap of the correlation between the expression levels of DEMORGs and the infiltration proportions of immune cells (Spearman correlation coefficient). **P*<0.05, ***P*<0.01, ****P*<0.001.

Abbreviations: IQR, interquartile range; ns, no significance.

LASSO and SVM-RFE were intersected, and finally CPT1A, EPHX2, and PRDX4 were obtained as UC feature genes related to MD and OS (Figure 5A–C).

MD and OS-Related Feature Genes Have Good Diagnostic Value for UC

As presented in Figure 5D, the expression of CPT1A and EPHX2 in the UC group was significantly lower than that in the HC group (both $P<0.001$), while the expression of PRDX4 was significantly higher than that in the HC group ($P<0.001$). The ROC curves indicated that CPT1A (AUC=0.982), EPHX2 (AUC=0.882), and PRDX4 (AUC=0.894) all had good diagnostic efficacy for UC (Figure 5E). The above results were validated in the GSE206285 dataset (Figure 5F and G). Furthermore, we constructed a nomogram for UC diagnosis based on these three feature genes (Figure 6A), and the ROC curve, calibration curve, and DCA demonstrated that the nomogram has good predictive performance (Figure 6B–D).

The Expression Levels of MD and OS-Related Feature Genes were Significantly Associated with the Clinical Activity of UC

The expression levels of the three feature genes were significantly correlated with Mayo scores (Figure 7A–C), with CPT1A ($r=-0.28$, $P<0.001$) and EPHX2 ($r=-0.38$, $P<0.001$) showing negative correlations, and PRDX4 ($r=0.40$, $P<0.001$) showing a positive correlation. In UC patients treated with golimumab, the response group exhibited a significant decrease in Mayo scores at week 6 ($P<0.001$), along with a trend toward increased EPHX2 expression ($P<0.05$) and decreased PRDX4 expression ($P<0.01$) (Figure 7D and E). However, in the non-response group, there were no significant differences in Mayo scores or the expression levels of the feature genes between week 6 and week 0 (Figure 7F and G).

Experimental Validation of MD and OS-Related Feature Gene Expression

The results of immunohistochemical staining showed that the protein expression levels of CPT1A and EPHX2 in the intestinal biopsy tissues of UC patients were significantly lower than those of controls (both $P<0.001$), while the protein expression level of PRDX4 was significantly higher than that of controls ($P<0.001$) (Figure 8). This is consistent with the results of bioinformatics analysis.

Discussion

The identification of UC biomarkers related to immune cell infiltration, disease activity, and therapeutic response may offer valuable references for the precision diagnosis and treatment of UC.[22,23] In this study, nine DEMORGs were first identified, based on which UC samples were clustered, and the correlation between DEMORGs and immune cell infiltration was analyzed. Secondly, three MD and OS-related feature genes with diagnostic value for UC were screened by machine learning, and a diagnostic nomogram was constructed. Finally, the protein expression levels of the feature genes were verified in tissue sections.

Among the nine DEMORGs, PRDX4 and SOD2 were upregulated genes primarily involved in the detoxification of ROS;[24,25] the remaining seven were downregulated genes closely associated with mitochondrial metabolic functions, such as glucose metabolism, fatty acid metabolism, and oxidative phosphorylation (OXPHOS).[26–28] Subtype C2 identified through unsupervised clustering had lower mitochondrial function scores and higher disease activity, thus justifying the classification and further illustrating the association between MD and UC disease activity. MD involves an increase in ROS, suppression of OXPHOS, and a decrease in the NAD/NADH ratio.[29] ROS levels exceeding physiological thresholds can cause cellular damage and further induce necroptosis or pyroptosis.[16,30] Meanwhile, DAMPs released after cell death, such as mtDNA, can promote immune cell recruitment and inflammatory responses.[6,31] The suppression of OXPHOS in IECs is not conducive to the maintenance of a physiological hypoxic environment at the epithelial-lumen interface, leading to a reduction in the abundance of obligate anaerobic bacteria that ferment dietary fibers into short-chain fatty acids (SCFAs).[32] NAD deficiency reduces the activity of mitochondrial homeostasis regulators sirtuin 1 (SIRT1) and SIRT3, thereby affecting mitochondrial biogenesis and antioxidant responses.[33,34] Therefore, MD is closely associated with typical UC manifestations, such as mucosal inflammation, epithelial barrier damage, and gut microbiota dysbiosis.

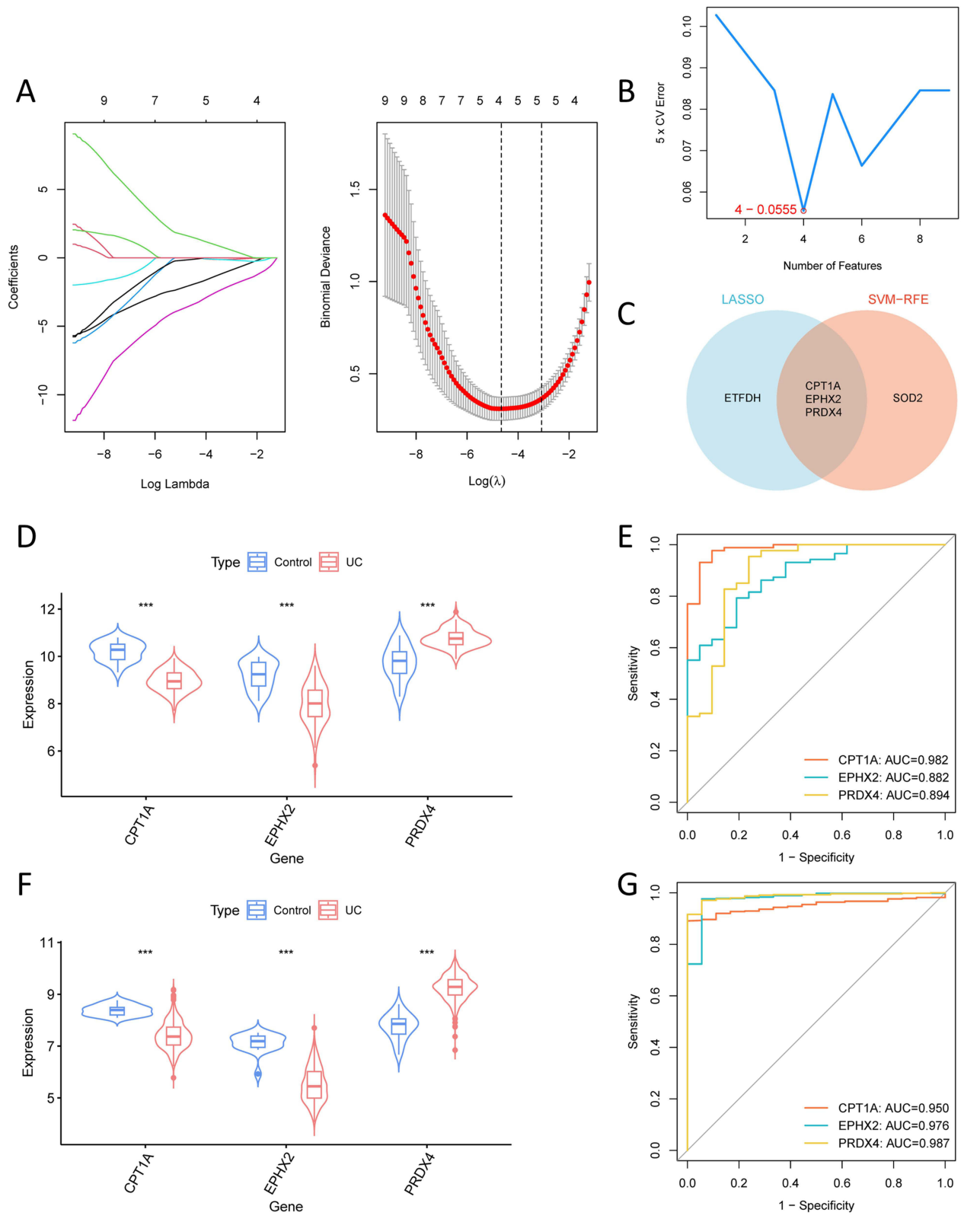

Figure 5 Machine learning screening for feature genes. (**A**) Coefficient path and optimal lambda selection in LASSO regression. (**B**) Cross-validation error in SVM-RFE algorithm. (**C**) Venn diagram: the intersection of LASSO and SVM-RFE results is the feature genes. (**D**) Violin plot comparing the expression levels of feature genes between UC patients and healthy controls in the training set (median [IQR], Wilcoxon test). (**E**) ROC curves showing the diagnostic performance of feature genes in the training set. (**F**) Violin plot comparing the expression levels of feature genes between UC patients and healthy controls in the validation set (median [IQR], Wilcoxon test). (**G**) ROC curves showing the diagnostic performance of feature genes in the validation set. ***$P<0.001$.

Abbreviations: LASSO, Least Absolute Shrinkage and Selection Operator; SVM-RFE, Support Vector Machine-Recursive Feature Elimination; UC, ulcerative colitis; IQR, interquartile range; ROC, receiver operating characteristic; AUC, area under the curve.

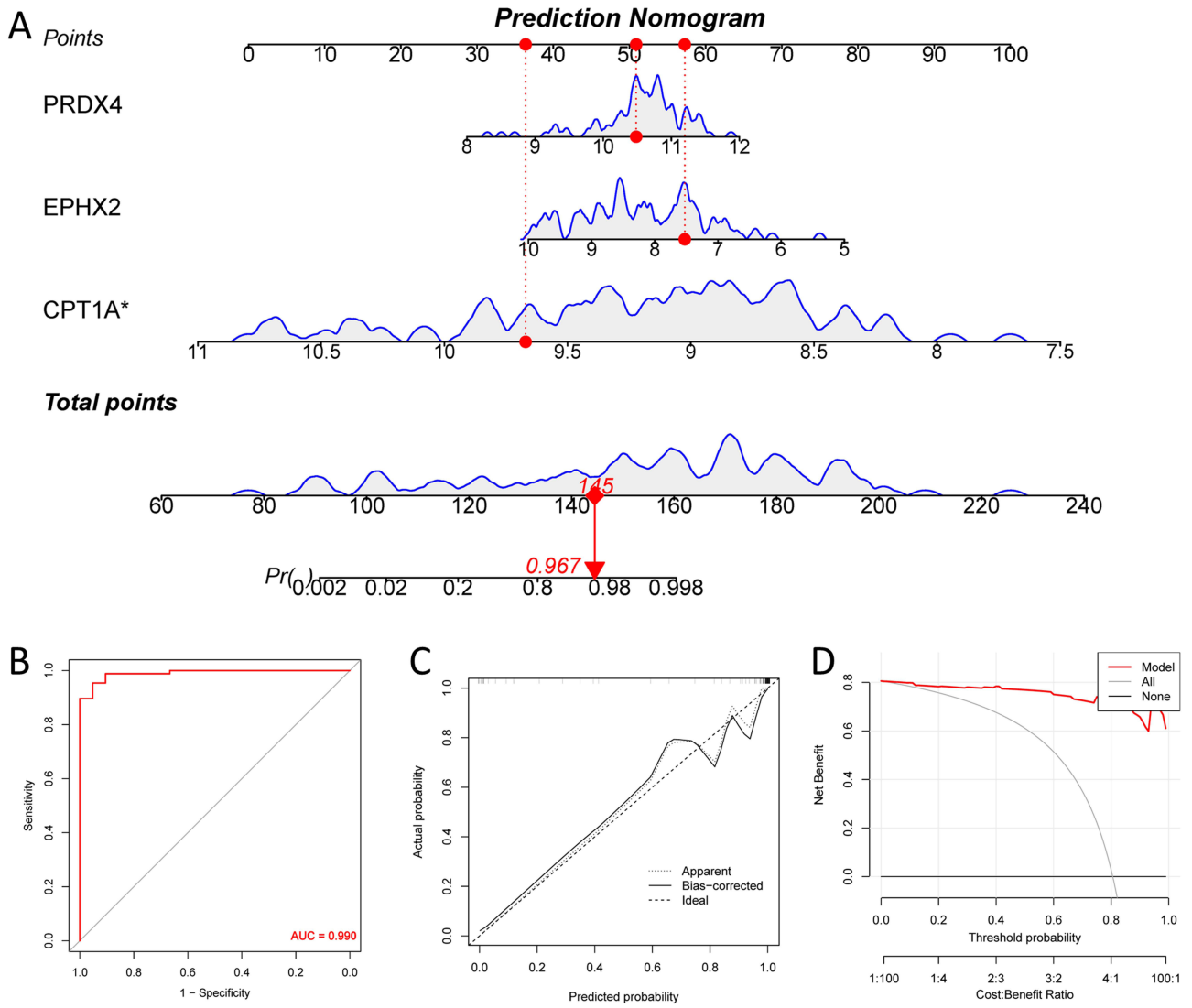

Figure 6 Diagnostic nomogram for UC. (**A**) Nomogram. (**B**) ROC curve. (**C**) Calibration curve. (**D**) Decision curve analysis.
Abbreviation: UC, ulcerative colitis.

Immune dysregulation is a key factor in the initiation and perpetuation of UC inflammation.[35] In recent years, the role of Tfh cells in the pathogenesis of UC has gained increasing attention, especially regarding their imbalance with follicular regulatory T (Tfr) cells and their interaction with DCs.[36,37] The immune cell infiltration assessment in this study also showed consistent results, indicating significantly higher infiltration of Tfh cells and activated DCs in the UC group or subtype C2. However, whether MD and OS are involved in the Tfh/Tfr imbalance remains unclear. Additionally, we found that the infiltration of M1 macrophages increased while that of M2 macrophages decreased in the UC group or subtype C2. It is widely recognized that M1 is the pro-inflammatory macrophage phenotype, while M2 is the anti-inflammatory phenotype.[38] Studies have shown that mitochondrial ROS can promote macrophage polarization towards the M1 type.[10] Moreover, macrophage polarization involves metabolic reprogramming, as many typical functions of M1 macrophages depend on glycolysis, whereas M2 macrophages rely more on OXPHOS.[39] Thus, MD in macrophages may contribute to M1 polarization.

Regarding the three MD and OS-related feature genes identified through machine learning, current research has not fully elucidated their specific roles in the onset or progression of UC. CPT1A is associated with mitochondrial fatty acid metabolism, encoding carnitine palmitoyltransferase 1, which is located on the outer mitochondrial membrane and acts as the rate-limiting enzyme in the β-oxidation of long-chain fatty acids.[27] A previous bioinformatics analysis by Alghamdi

https://doi.org/10.2147/JIR.S506851

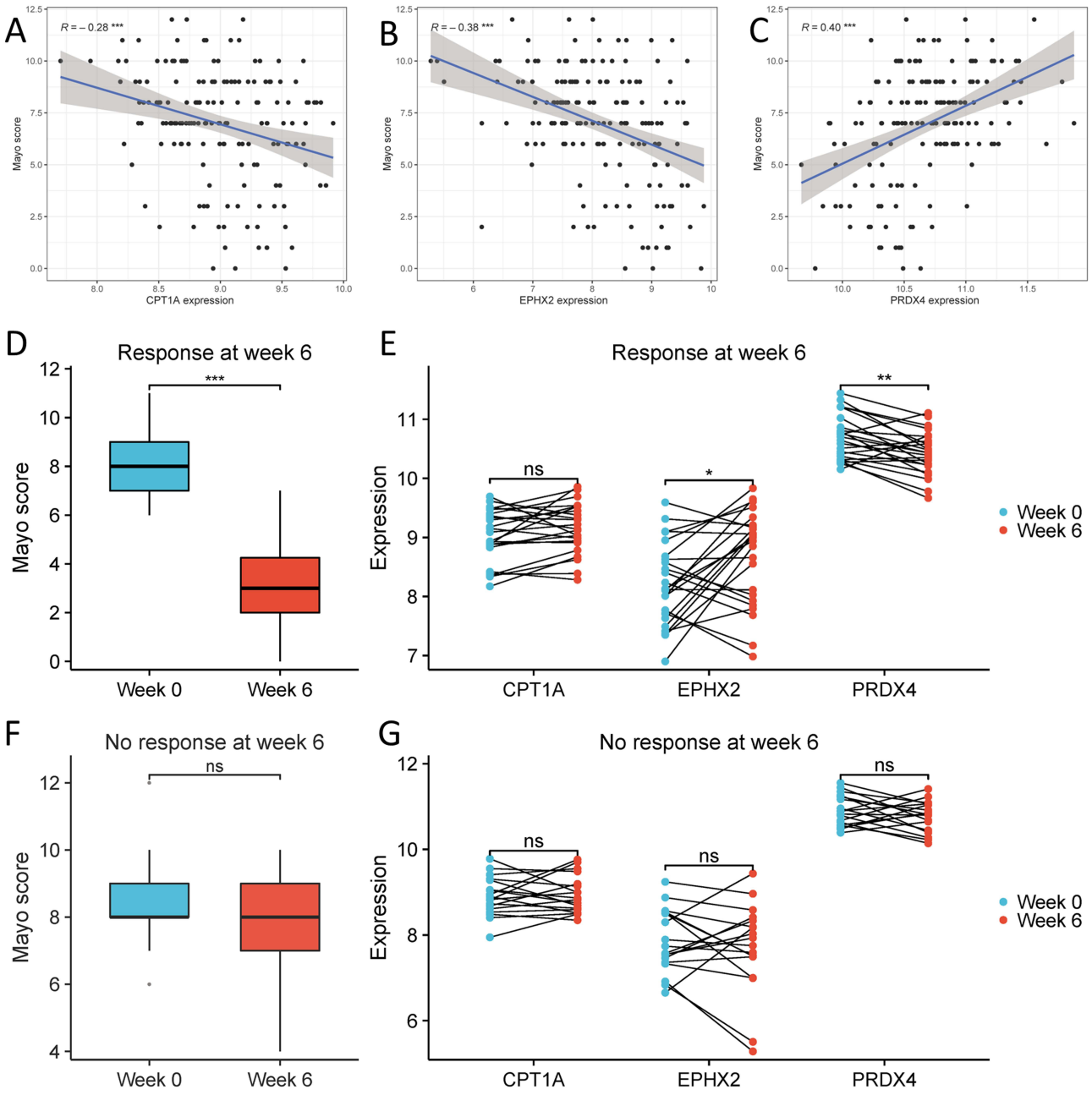

Figure 7 Correlation analysis between feature genes and disease activity. (**A–C**) Correlation analysis between the expression levels of feature genes and Mayo scores (Spearman correlation coefficient). (**D**) Boxplot comparing Mayo scores at week 0 and week 6 in the golimumab response group (median [IQR], Wilcoxon test). (**E**) Paired comparison of feature gene expression levels at week 0 and week 6 in the golimumab response group (paired *t*-test). (**F**) Boxplot comparing Mayo scores at week 0 and week 6 in the golimumab non-response group (median [IQR], Wilcoxon test). (**G**) Paired comparison of feature gene expression levels at week 0 and week 6 in the golimumab non-response group (paired *t*-test). **P*<0.05, ***P*<0.01, ****P*<0.001.

Abbreviations: IQR, interquartile range; ns, no significance.

et al reported that CPT1A is a key gene associated with IBD.[40] Since the energy supply and functional maintenance of certain immune cells rely on fatty acid oxidation (FAO), the role of CPT1A in immune cell differentiation has attracted considerable attention. Inducible regulatory T (iTreg) cells are a subset of Treg cells and are essential for maintaining intestinal immune homeostasis.[41] Research by Hao et al demonstrated that butyrate facilitates FAO and iTreg cell differentiation by upregulating CPT1A activity.[42] A recent study by Li et al revealed that the gut microbial metabolite indole-3-propionic acid alleviates colitis by inducing M2 macrophage polarization, a process mediated by CPT1A upregulation and enhanced FAO.[43] EPHX2 encodes soluble epoxide hydrolase (sEH), a bifunctional enzyme with

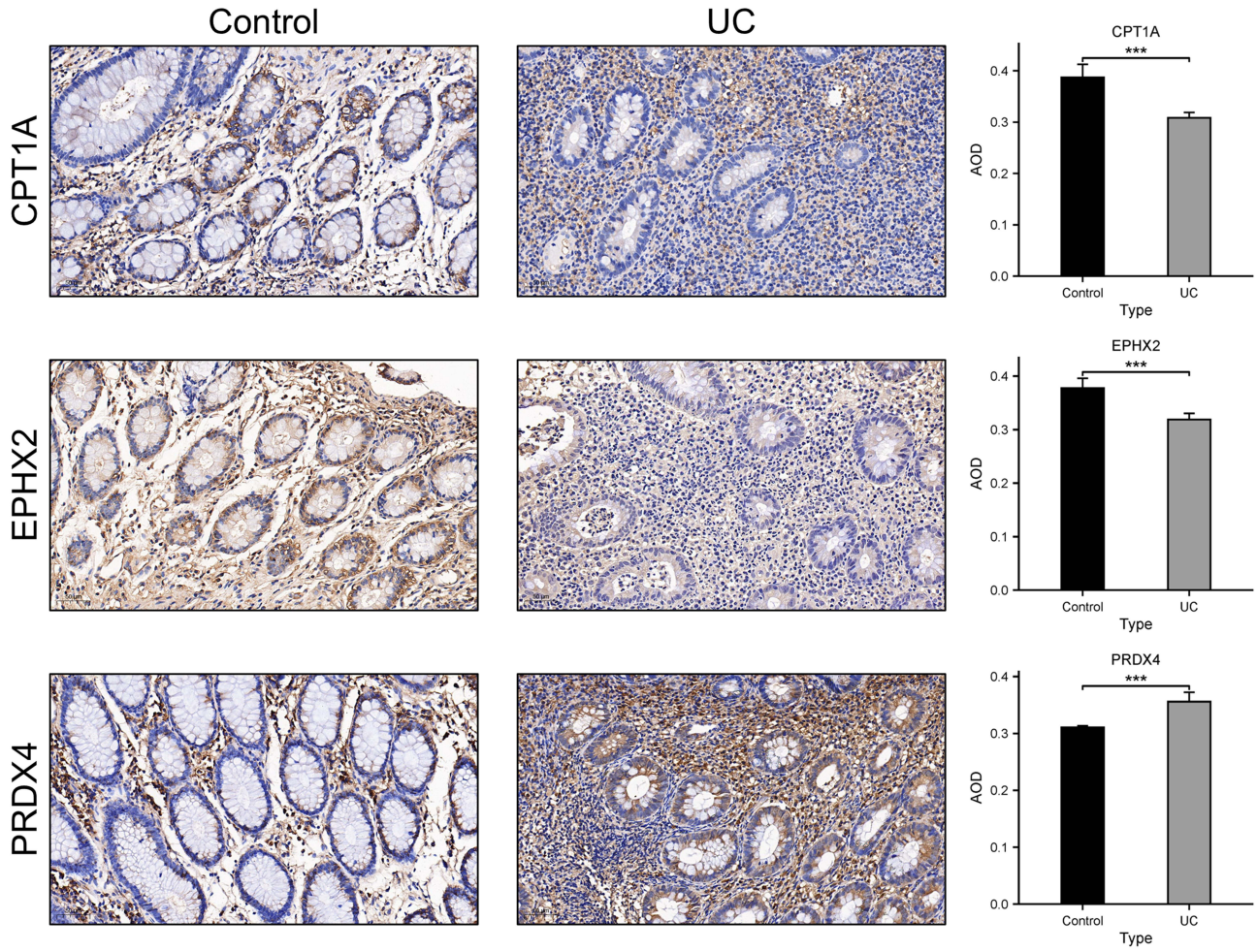

Figure 8 Immunohistochemical staining of proteins encoded by feature genes in colonoscopic biopsy tissues from UC patients and controls (mean±SD, *t*-test). ****P*<0.001.
Abbreviations: UC, ulcerative colitis; AOD, average optical density; SD, standard deviation.

epoxide hydrolase activity in its C-terminal domain and lipid phosphatase activity in its N-terminal domain.[44] Epoxyeicosatrienoic acids (EETs), derived from arachidonic acid metabolism via cytochrome P450 enzymes, are recognized as anti-inflammatory mediators, whereas sEH is the hydrolase of EETs.[45] Qiu et al were the first to investigate the levels of EETs and sEH in intestinal tissues of UC patients and found that EETs concentrations were elevated while sEH expression was reduced in inflamed tissues compared to adjacent non-inflammatory tissues, suggesting that increased EETs levels may be part of the protective mechanism in UC.[46] Reisdorf et al did not observe a statistically significant difference in EPHX2 protein expression levels between UC colonic biopsy samples and healthy controls using Western blot analysis.[47] However, treatment with the sEH inhibitor (GSK1910364) alleviated dextran sulfate sodium (DSS)-induced colitis in mice.[47] It is currently considered that sEH inhibitors exert their effects through EETs-mediated regulation of mitochondrial function, reduction of ROS levels, and inhibition of endoplasmic reticulum stress.[48] PRDX4 encodes peroxiredoxin 4, which is primarily localized in the endoplasmic reticulum and has a dual function in hydrogen peroxide degradation and protein oxidative folding.[49] It has been investigated in multiple diseases. For example, a cohort study by Geertsema et al identified serum peroxiredoxin 4 as an OS biomarker associated with the risk of chronic kidney disease.[50] Research by Huang et al found that peroxiredoxin 4 mitigates diabetic retinopathy by suppressing endoplasmic reticulum stress, OS, and MD in Müller cells.[51] In the field of colitis, animal studies have shown that PRDX4 knockout exacerbates DSS-induced colonic mucosal injury.[52] Additionally, peroxiredoxin 4 directly regulates IL-1β release by restricting caspase-1 activity.[53] Therefore, CPT1A, EPHX2, and PRDX4 all have promising research prospects in UC.

https://doi.org/10.2147/JIR.S506851

Considering the close association between MD and OS, this study comprehensively analyzed the molecular subtypes, immune infiltration characteristics, and feature genes related to MD and OS in UC, offering new insights into biomarker identification and therapeutic strategy development. However, this study still has some limitations. First, there is a lack of exploration into the specific mechanisms by which the proteins encoded by the feature genes participate in immune regulation and inflammatory response, which requires further research for clarification. Second, although colonoscopic biopsy tissues from UC patients and controls were collected, the sample size is relatively small. Finally, the current study did not analyze the degree of MD, OS levels, or the expression of feature genes in specific cell types.

Conclusions

CPT1A, EPHX2, and PRDX4 are feature genes related to MD and OS in UC, and their expression levels are significantly associated with the proportion of immune cell infiltration and disease activity. This study provides valuable insights into the role of MD and OS in UC.

Data Sharing Statement

GSE92415 and GSE206285 datasets can be downloaded from the Gene Expression Omnibus (https://www.ncbi.nlm.nih.gov/geo/). Mitochondrial-related genes can be downloaded from the Human MitoCarta3.0 database (https://www.broadinstitute.org/mitocarta/). Oxidative stress-related genes can be obtained from the Molecular Signatures Database (http://www.gsea-msigdb.org/gsea/downloads.jsp) and GeneCards database (https://www.genecards.org/).

Ethics Approval and Consent to Participate

This study has been approved by the Ethics Committee of Renmin Hospital of Wuhan University (WDRY 2022-K130), and all participants have signed an informed consent form.

Acknowledgments

We would like to thank all the contributors to the Gene Expression Omnibus, Human MitoCarta3.0 database, Molecular Signatures Database, and GeneCards database.

Author Contributions

All authors made a significant contribution to the work reported, whether that is in the conception, study design, execution, acquisition of data, analysis and interpretation, or in all these areas; took part in drafting, revising or critically reviewing the article; gave final approval of the version to be published; have agreed on the journal to which the article has been submitted; and agree to be accountable for all aspects of the work.

Funding

The study was supported by the National Natural Science Foundation of China (No. 82370542).

Disclosure

The authors have no conflicts of interest to declare in this work.

References

1. Ungaro R, Mehandru S, Allen PB, Peyrin-Biroulet L, Colombel JF. Ulcerative colitis. *Lancet*. 2017;389(10080):1756–1770. doi:10.1016/S0140-6736(16)32126-2
2. Ramos GP, Papadakis KA. Mechanisms of disease: inflammatory bowel diseases. *Mayo Clin Proc*. 2019;94(1):155–165. doi:10.1016/j.mayocp.2018.09.013
3. Buie MJ, Quan J, Windsor JW, et al. Global hospitalization trends for Crohn's disease and ulcerative colitis in the 21st Century: a systematic review with temporal analyses. *Clin Gastroenterol Hepatol*. 2023;21(9):2211–2221. doi:10.1016/j.cgh.2022.06.030
4. Agrawal M, Spencer EA, Colombel JF, Ungaro RC. Approach to the management of recently diagnosed inflammatory bowel disease patients: a user's guide for adult and pediatric gastroenterologists. *Gastroenterology*. 2021;161(1):47–65. doi:10.1053/j.gastro.2021.04.063

5. Lasa JS, Olivera PA, Danese S, Peyrin-Biroulet L. Efficacy and safety of biologics and small molecule drugs for patients with moderate-to-severe ulcerative colitis: a systematic review and network meta-analysis. *Lancet Gastroenterol Hepatol*. 2022;7(2):161–170. doi:10.1016/S2468-1253(21)00377-0
6. Boyapati RK, Dorward DA, Tamborska A, et al. Mitochondrial DNA is a pro-inflammatory damage-associated molecular pattern released during active IBD. *Inflamm Bowel Dis*. 2018;24(10):2113–2122. doi:10.1093/ibd/izy095
7. Santhanam S, Rajamanickam S, Motamarry A, et al. Mitochondrial electron transport chain complex dysfunction in the colonic mucosa in ulcerative colitis. *Inflamm Bowel Dis*. 2012;18(11):2158–2168. doi:10.1002/ibd.22926
8. Cunningham KE, Vincent G, Sodhi CP, et al. Peroxisome proliferator-activated receptor-γ coactivator 1-α (PGC1α) protects against experimental murine colitis. *J Biol Chem*. 2016;291(19):10184–10200. doi:10.1074/jbc.M115.688812
9. West AP, Shadel GS. Mitochondrial DNA in innate immune responses and inflammatory pathology. *Nat Rev Immunol*. 2017;17(6):363–375. doi:10.1038/nri.2017.21
10. Mills EL, Kelly B, Logan A, et al. Succinate dehydrogenase supports metabolic repurposing of mitochondria to drive inflammatory macrophages. *Cell*. 2016;167(2):457–470.e13. doi:10.1016/j.cell.2016.08.064
11. Turrens JF. Mitochondrial formation of reactive oxygen species. *J Physiol*. 2003;552(Pt 2):335–344. doi:10.1113/jphysiol.2003.049478
12. Sena LA, Chandel NS. Physiological roles of mitochondrial reactive oxygen species. *Mol Cell*. 2012;48(2):158–167. doi:10.1016/j.molcel.2012.09.025
13. Ho GT, Theiss AL. Mitochondria and inflammatory bowel diseases: toward a stratified therapeutic intervention. *Annu Rev Physiol*. 2022;84:435–459. doi:10.1146/annurev-physiol-060821-083306
14. Geertsema S, Bourgonje AR, Fagundes RR, et al. The NRF2/Keap1 pathway as a therapeutic target in inflammatory bowel disease. *Trends Mol Med*. 2023;29(10):830–842. doi:10.1016/j.molmed.2023.07.008
15. Sahoo DK, Heilmann RM, Paital B, et al. Oxidative stress, hormones, and effects of natural antioxidants on intestinal inflammation in inflammatory bowel disease. *Front Endocrinol*. 2023;14:1217165. doi:10.3389/fendo.2023.1217165
16. Yang X, Li G, Lou P, et al. Excessive nucleic acid R-loops induce mitochondria-dependent epithelial cell necroptosis and drive spontaneous intestinal inflammation. *Proc Natl Acad Sci U S A*. 2024;121(1):e2307395120. doi:10.1073/pnas.2307395120
17. Wen X, Tang L, Zhong R, Liu L, Chen L, Zhang H. Role of mitophagy in regulating intestinal oxidative damage. *Antioxidants*. 2023;12(2):480. doi:10.3390/antiox12020480
18. Zhang YF, Fan MY, Bai QR, et al. Precision therapy for ulcerative colitis: insights from mitochondrial dysfunction interacting with the immune microenvironment. *Front Immunol*. 2024;15:1396221. doi:10.3389/fimmu.2024.1396221
19. Li Q, Liu Y, Li B, et al. Bioinformatics analysis of oxidative stress genes in the pathogenesis of ulcerative colitis based on a competing endogenous RNA regulatory network. *PeerJ*. 2024;12:e17213. doi:10.7717/peerj.17213
20. Sandborn WJ, Feagan BG, Marano C, et al. Subcutaneous golimumab induces clinical response and remission in patients with moderate-to-severe ulcerative colitis. *Gastroenterology*. 2014;146(1):85–95;quize e14–5. doi:10.1053/j.gastro.2013.05.048
21. Pavlidis P, Tsakmaki A, Pantazi E, et al. Interleukin-22 regulates neutrophil recruitment in ulcerative colitis and is associated with resistance to ustekinumab therapy. *Nat Commun*. 2022;13(1):5820. doi:10.1038/s41467-022-33331-8
22. Huo A, Wang F. Biomarkers of ulcerative colitis disease activity CXCL1, CYP2R1, LPCAT1, and NEU4 and their relationship to immune infiltrates. *Sci Rep*. 2023;13(1):12126. doi:10.1038/s41598-023-39012-w
23. Motawi TK, Shaker OG, Amr G, Senousy MA. RNA methylation machinery and m(6)A target genes as circulating biomarkers of ulcerative colitis and Crohn's disease: correlation with disease activity, location, and inflammatory cytokines. *Clin Chim Acta*. 2024;561:119831. doi:10.1016/j.cca.2024.119831
24. Wood ZA, Schröder E, Robin Harris J, Poole LB. Structure, mechanism and regulation of peroxiredoxins. *Trends Biochem Sci*. 2003;28(1):32–40. doi:10.1016/S0968-0004(02)00003-8
25. Flynn JM, Melov S. SOD2 in mitochondrial dysfunction and neurodegeneration. *Free Radic Biol Med*. 2013;62:4–12. doi:10.1016/j.freeradbiomed.2013.05.027
26. Go Y, Jeong JY, Jeoung NH, et al. Inhibition of pyruvate dehydrogenase kinase 2 protects against hepatic steatosis through modulation of tricarboxylic acid cycle anaplerosis and ketogenesis. *Diabetes*. 2016;65(10):2876–2887. doi:10.2337/db16-0223
27. Gobin S, Thuillier L, Jogl G, et al. Functional and structural basis of carnitine palmitoyltransferase 1A deficiency. *J Biol Chem*. 2003;278(50):50428–50434. doi:10.1074/jbc.M310130200
28. Herrero Martín JC, Salegi Ansa B, Álvarez-rivera G, et al. An ETFDH-driven metabolon supports OXPHOS efficiency in skeletal muscle by regulating coenzyme Q homeostasis. *Nat Metab*. 2024;6(2):209–225. doi:10.1038/s42255-023-00956-y
29. Haque PS, Kapur N, Barrett TA, Theiss AL. Mitochondrial function and gastrointestinal diseases. *Nat Rev Gastroenterol Hepatol*. 2024;21(8):537–555. doi:10.1038/s41575-024-00931-2
30. Wang J, Wu Z, Zhu M, Zhao Y, Xie J. ROS induced pyroptosis in inflammatory disease and cancer. *Front Immunol*. 2024;15:1378990. doi:10.3389/fimmu.2024.1378990
31. Zhong Z, Liang S, Sanchez-Lopez E, et al. New mitochondrial DNA synthesis enables NLRP3 inflammasome activation. *Nature*. 2018;560(7717):198–203. doi:10.1038/s41586-018-0372-z
32. Litvak Y, Byndloss MX, Bäumler AJ. Colonocyte metabolism shapes the gut microbiota. *Science*. 2018;362(6418): eaat9076. doi:10.1126/science.aat9076
33. Novak EA, Crawford EC, Mentrup HL, et al. Epithelial NAD(+) depletion drives mitochondrial dysfunction and contributes to intestinal inflammation. *Front Immunol*. 2023;14:1231700. doi:10.3389/fimmu.2023.1231700
34. Ji Z, Liu GH, Qu J. Mitochondrial sirtuins, metabolism, and aging. *J Genet Genomics*. 2022;49(4):287–298. doi:10.1016/j.jgg.2021.11.005
35. Le Berre C, Honap S, Peyrin-Biroulet L. Ulcerative colitis. *Lancet*. 2023;402(10401):571–584. doi:10.1016/S0140-6736(23)00966-2
36. Wang X, Zhu Y, Zhang M, et al. The shifted balance between circulating follicular regulatory T cells and follicular helper T cells in patients with ulcerative colitis. *Clin Sci*. 2017;131(24):2933–2945. doi:10.1042/CS20171258
37. Bai X, Chen S, Chi X, et al. Reciprocal regulation of T follicular helper cells and dendritic cells drives colitis development. *Nat Immunol*. 2024;25(8):1383–1394. doi:10.1038/s41590-024-01882-1
38. Murray PJ. Macrophage polarization. *Annu Rev Physiol*. 2017;79:541–566. doi:10.1146/annurev-physiol-022516-034339

39. Viola A, Munari F, Sánchez-Rodríguez R, Scolaro T, Castegna A. The metabolic signature of macrophage responses. *Front Immunol*. 2019;10:1462. doi:10.3389/fimmu.2019.01462
40. Alghamdi KS, Kassar RH, Farrash WF, et al. Key disease-related genes and immune cell infiltration landscape in inflammatory bowel disease: a bioinformatics investigation. *Int J mol Sci*. 2024;25(17):9751. doi:10.3390/ijms25179751
41. Josefowicz SZ, Lu LF, Rudensky AY. Regulatory T cells: mechanisms of differentiation and function. *Annu Rev Immunol*. 2012;30:531–564. doi:10.1146/annurev.immunol.25.022106.141623
42. Hao F, Tian M, Zhang X, et al. Butyrate enhances CPT1A activity to promote fatty acid oxidation and iTreg differentiation. *Proc Natl Acad Sci U S A*. 2021;118(22): e2014681118. doi:10.1073/pnas.2014681118
43. Li J, Zou P, Xiao R, Wang Y. Indole-3-propionic acid alleviates DSS-induced colitis in mice through macrophage glycolipid metabolism. *Int Immunopharmacol*. 2025;152:114388. doi:10.1016/j.intimp.2025.114388
44. Newman JW, Morisseau C, Harris TR, Hammock BD. The soluble epoxide hydrolase encoded by EPXH2 is a bifunctional enzyme with novel lipid phosphate phosphatase activity. *Proc Natl Acad Sci U S A*. 2003;100(4):1558–1563. doi:10.1073/pnas.0437724100
45. Morisseau C, Hammock BD. Impact of soluble epoxide hydrolase and epoxyeicosanoids on human health. *Annu Rev Pharmacol Toxicol*. 2013;53:37–58. doi:10.1146/annurev-pharmtox-011112-140244
46. Qiu YE, Qin J, Luo Y, et al. Increased epoxyeicosatrienoic acids may be part of a protective mechanism in human ulcerative colitis, with increased CYP2J2 and reduced soluble epoxide hydrolase expression. *Prostaglandins Other Lipid Mediat*. 2018;136:9–14. doi:10.1016/j.prostaglandins.2018.03.004
47. Reisdorf WC, Xie Q, Zeng X, et al. Preclinical evaluation of EPHX2 inhibition as a novel treatment for inflammatory bowel disease. *PLoS One*. 2019;14(4):e0215033. doi:10.1371/journal.pone.0215033
48. Inceoglu B, Bettaieb A, Haj FG, Gomes AV, Hammock BD. Modulation of mitochondrial dysfunction and endoplasmic reticulum stress are key mechanisms for the wide-ranging actions of epoxy fatty acids and soluble epoxide hydrolase inhibitors. *Prostaglandins Other Lipid Mediat*. 2017;133:68–78. doi:10.1016/j.prostaglandins.2017.08.003
49. Fujii J, Ochi H, Yamada S. A comprehensive review of peroxiredoxin 4, a redox protein evolved in oxidative protein folding coupled with hydrogen peroxide detoxification. *Free Radic Biol Med*. 2025;227:336–354. doi:10.1016/j.freeradbiomed.2024.12.015
50. Geertsema S, Geertsema P, Kieneker LM, et al. Serum peroxiredoxin-4, a biomarker of oxidative stress, associates with new-onset chronic kidney disease: a population-based cohort study. *Redox Biol*. 2024;77:103408. doi:10.1016/j.redox.2024.103408
51. Huang Y, Zhang Y, Liu Y, Jin Y, Yang H. PRDX4 mitigates diabetic retinopathy by inhibiting reactive gliosis, apoptosis, ER stress, oxidative stress, and mitochondrial dysfunction in Müller cells. *J Biol Chem*. 2025;301(1):108111. doi:10.1016/j.jbc.2024.108111
52. Takagi T, Homma T, Fujii J, et al. Elevated ER stress exacerbates dextran sulfate sodium-induced colitis in PRDX4-knockout mice. *Free Radic Biol Med*. 2019;134:153–164. doi:10.1016/j.freeradbiomed.2018.12.024
53. Lipinski S, Pfeuffer S, Arnold P, et al. Prdx4 limits caspase-1 activation and restricts inflammasome-mediated signaling by extracellular vesicles. *EMBO J*. 2019;38(20):e101266. doi:10.15252/embj.2018101266